Hybrid green LEDs based on *n*-ZnO/(InGaN/GaN) multi-quantum-wells/*p*-GaN

C. Bayram,[a] F. Hosseini Teherani,[b,†] D. J. Rogers,[b] and M. Razeghi [*a]
[a]Center for Quantum Devices, Department of Electrical Engineering and Computer Science, Northwestern University, Evanston, Illinois, USA 60208 ;
[b]Nanovation SARL, 103 bis Rue de Versailles, Orsay 91400, France

ABSTRACT

Hybrid green light-emitting diodes (LEDs) comprised of *n*-ZnO/(InGaN/GaN) multi-quantum-wells/*p*-GaN were grown on semi-insulating AlN/sapphire using pulsed laser deposition for the *n*-ZnO and metal organic chemical vapor deposition for the other layers. X-ray diffraction revealed that high crystallographic quality was preserved after the *n*-ZnO growth. LEDs showed a turn-on voltage of 2.5 V and a room temperature electroluminescence (EL) centered at 510 nm. A blueshift and narrowing of the EL peak with increasing current was attributed to bandgap renormalization. The results indicate that hybrid LED structures could hold the prospect for the development of green LEDs with superior performance.

Keywords: pulsed laser deposition, metalorganic chemical vapor deposition, ZnO, InGaN/GaN multi-quantum wells, green light-emitting diode

1. INTRODUCTION

1.1 Solid State Lighting

Solid state lighting (SSL) holds the promise of a more energy-efficient, longer-lasting, more compact, and lower maintenance substitute for today's incandescent and fluorescent light sources. Since lighting currently represents about 22% of all electricity consumption, the adoption of SSL could significantly reduce greenhouse gas emissions. [1] Light-emitting diodes (LEDs), based on the InGaN alloy, are currently the most promising candidates for realizing SSL. InGaN is a direct wide bandgap semiconductor with an emission that can span the entire visible spectrum via compositional tuning. However, InGaN LED performance remains wavelength-dependent. Indeed, ultrabright and efficient blue InGaN-based LEDs are readily available[2] but the performance of InGaN-based green LEDs is still far from adequate for use in SSL.[3, 4, 5]

1.2 Conventional III-nitride green emitters and motivation for ZnO hybridization

The higher indium content required in the active layers for green emission causes problems. First, the limited solubility of indium in InGaN [6] imposes a restricted growth window for the green-emitting InGaN active layer. Second, InGaN with high indium content becomes unstable at elevated substrate temperature (T_s).[7] Conventionally, a *p*-GaN layer is grown on top of an InGaN multi-quantum-well (MQW) active layer. The *p*-GaN layer is grown at significantly higher T_s than the InGaN MQW active layer in order to obtain high structural quality. This leads, however, to indium leaking out of the active layers, which reduces the LED output.[4, 7] Thus, it is important to combat indium diffusion in order to obtain InGaN-based green LEDs with superior performance.

In conventional GaN-based LEDs, the *p*-layer is deposited on top of the *n*-layer because the *n*-layer can be grown with higher crystallographic and morphological qualities than the *p*-layer. In this work, we adopted an inverted LED structure employing a *n*-ZnO layer grown on top of (InGaN/GaN) MQW/*p*-GaN/AlN/sapphire. Through the use of pulsed laser deposition (PLD), a high quality *n*-ZnO layer could be grown at significantly lower T_s than is typically required for GaN growth in metal organic chemical vapor deposition (MOCVD). This approach could be beneficial, particularly for green

† fht@nanovation.com; phone +33 650-81-0836; fax +33 1 64 46 29 49; http://www.nanovation.com
* razeghi@eecs.northwestern.edu; phone 1 (847) 491-7251; fax 1 (847) 476-1817; http://cqd.eecs.northwestern.edu

Zinc Oxide Materials and Devices IV, edited by Ferechteh Hosseini Teherani, Cole W. Litton, David J. Rogers,
Proc. of SPIE Vol. 7217, 72170P · © 2009 SPIE · CCC code: 0277-786X/09/$18 · doi: 10.1117/12.817033

light emitters,[8] in which the high indium content InGaN active layers are adversely affected by the high T_s required for the GaN growth. Furthermore, the refractive index of ZnO at 500 nm is 2.0 compared with 2.5 for GaN. Thus, lower critical angle loss is expected for light extraction through ZnO-capped LEDs. In this paper, we report the fabrication and the optical, structural, and electrical characteristics of these hybrid green LEDs.

ZnO is a wide bandgap material (E_g=3.3 eV) with a large exciton binding energy (60 meV). It has a low toxicity and the same wurtzite structure as GaN. The small in-plane lattice mismatch (~1.8%) with GaN makes ZnO a good candidate for integration in nitride devices. [9,10] Recently, there have been many reports of ultraviolet emitters based on *n*-ZnO/*p*-GaN heterostructures. [11,12,13] In this work, ZnO is adopted as the *n*-layer in a new kind of hybrid green LED.

2. EXPERIMENT

2.1 Material Growth and Characterization

The AlGaInN compounds were grown in an AIXTRON 200/4-HT horizontal flow low pressure MOCVD reactor. Trimethlyaluminum (TMAl), trimethlygallium (TMGa), trimethlyindium (TMIn), and bis(cyclopentadienyl)magnesium (DCpMg) were the metal organic cation precursors for Al, Ga, In, and Mg, respectively. Ammonia (NH_3) was used as the nitrogen source. Hydrogen was used as the carrier gas in the AlN and *p*-GaN layers.

p-GaN was grown on 600-nm-thick AlN on sapphire in order to improve the quality of the *p*-GaN.[14] Rapid thermal annealing was realized at 1000 °C for 30 s in order to activate the Mg dopant. Hole carrier concentration was determined to be 7.8×10^{17} cm^{-3} by Hall effect measurements. The surface of the *p*-GaN was chemically cleaned before the regrowth of the InGaN/GaN MQWs. A five period MQW structure was grown in a nitrogen ambient. Each period consisted of a 2-nm-thick InGaN quantum well with a 4-nm-thick GaN barrier. Finally, a *n*-ZnO layer[15] was grown on top of the (InGaN/GaN) MQW/*p*-GaN by PLD to complete the green LED.

ZnO was also simultaneously grown on sapphire for electrical characterization purposes. Room temperature (RT) Hall effect measurements were performed on the *n*-ZnO/sapphire in van der Pauw configuration with 400 Å Ti/300 Å Pt/1200 Å Au contacts. The contacts proved Ohmic and carrier concentration was determined to be 2.8×10^{19} cm^{-3} with a mobility of 10.0 $cm^2/V\cdot s$ and a resistivity of 0.02 $\Omega\cdot cm$. Photoluminescence (PL) measurements were carried out at RT with a frequency-doubled argon-ion laser at 244 nm. Room temperature PL for the *n*-ZnO/sapphire reference sample revealed a single peak at 377 nm corresponding to the *n*-ZnO band-edge. The spectrum also had relatively low green signal, which implies that there is a relatively low defect/dislocation density in the sample. Laser power dependent measurements showed no significant peak shift or full-width-at-half-maximum (FWHM) broadening. A linear increase in PL main peak intensity with increasing laser radiant power was observed. These results indicate high optical quality of the ZnO layer.

Figure 1(a) shows an SEM micrograph of the top surface of the *n*-ZnO layer of the fabricated hybrid LED. The surface morphology appears slightly rough (Fig. 1(a)). Figure 1(b) shows an SEM fracture cross-sectional image. The *n*-ZnO / MQW/ *p*-GaN/ AlN/ Sapphire (Al_2O_3) LED layers can clearly be distinguished.

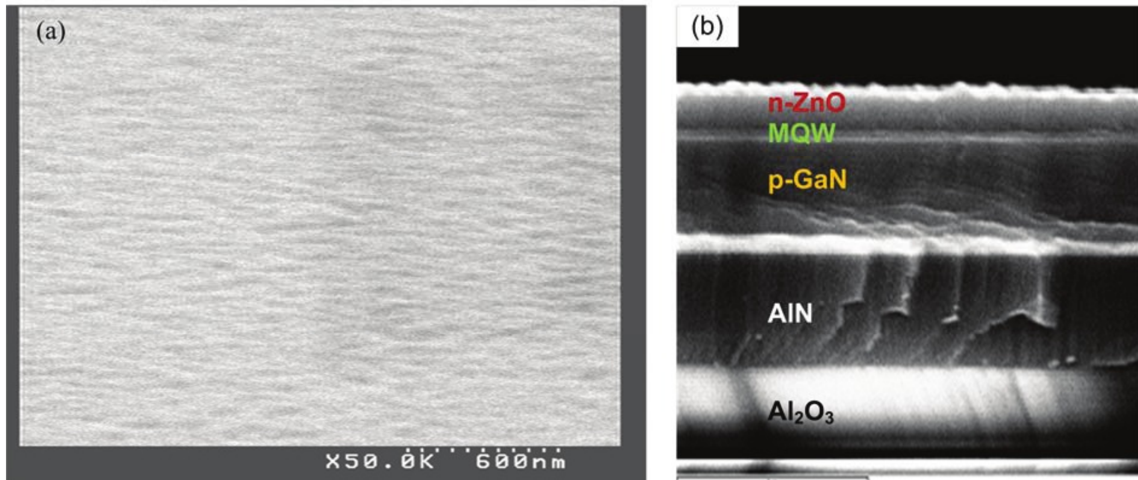

Fig. 1. SEM micrographs of the hybrid LED: (a) Surface and (b) Cross-sectional view.

Normalized RT photoluminescence (PL) spectra for the device layers are shown in Fig. 2. The spectrum for the *p*-GaN is dominated by 2.9 eV Mg-related peaks. [16] This band is commonly observed in *p*-GaN and is attributed to defect-related deep level centers. [17] The PL spectrum, once the InGaN/GaN MQWs were grown on the *p*-GaN, shows a strong emission peaked at 2.5 eV without the 2.9 eV Mg-related peaks. The multiple peaks in the spectrum are generated by a Fabry–Pérot cavity formed with the AlN-sapphire interface. The PL spectrum for the completed hybrid LED structure (including the *n*-ZnO top layer) shows the strongest main emission peak centered at 3.3 eV. This corresponds to the ZnO band edge. The relative intensity of the 2.5 eV emission from the InGaN/GaN MQW in this spectrum is lower than that for the spectrum prior to ZnO growth. This is mainly due to the impact of the higher ZnO main emission peak intensity on the spectrum normalization.

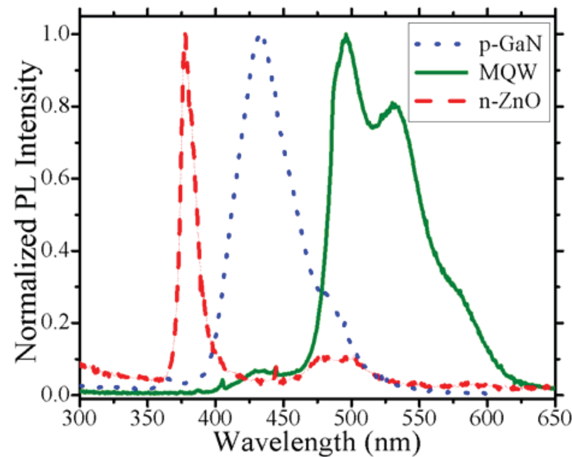

Fig. 2. RT normalized PL spectra as consecutive *p*-GaN, InGaN/GaN MQW, and *n*-ZnO layers were grown on AlN/Sapphire.

X-ray diffraction (XRD) studies were performed using a High Resolution Panalytical MPD-Pro system Diffractrometer. Figure 3 shows an x-ray diffraction (XRD) ω-2θ scan for the (0002) peak of the LED structure before- and after-ZnO growths. The ZnO and GaN peaks are indistinguishable suggesting a good lattice match. The full widths at half maximum (FWHMs) for the (0002) peaks before- and after-ZnO depositions are 253 and 259 arc sec, respectively. The MQW-related satellite peaks were similar before and after the ZnO growth. This indicates that the active layers

maintained their compositional and structural integrities. From the satellite peaks, the period of the active layer was determined to be 6.1 nm, which is in agreement with bulk growth calibrations.

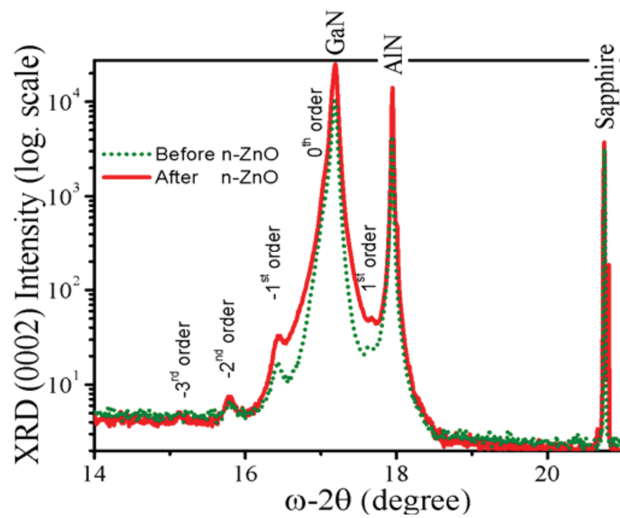

Fig. 3. RT XRD ω/2θ scans for the (0002) peak before- and after- growth of *n*-ZnO on the (InGaN/GaN) MQW/*p*-GaN/AlN/Sapphire.

2.2 Device Fabrication

Hybrid green LEDs were fabricated using conventional processing techniques. First of all, the samples were cleaned chemically. Then circular LED mesas with an area of 0.30 mm^2 were fabricated by masking the surface and dry etching right through the ZnO layer to a depth of 500 nm into the *p*-GaN (see Fig. 4(a)). 30 Å Ni/30 Å Au/400 Å Ti/1200 Å Au and 400 Å Ti/300 Å Pt/1200 Å Au contacts were evaporated onto the *p*-GaN and *n*-ZnO, respectively (Fig. 4(b)). SEM micrographs of a fabricated hybrid LED is shown in Fig. 4. The inset of Fig. 5(a) also illustrates the device structure. The effects of solvents, annealing and etching on *n*-ZnO will be discussed elsewhere. [18]

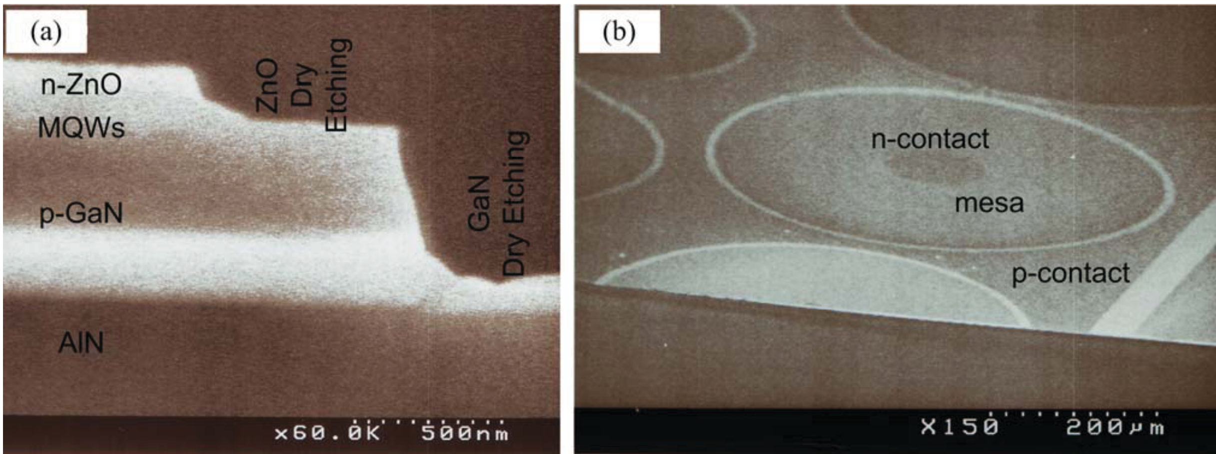

Fig. 4. SEM micrographs of a fabricated hybrid LED (a) Side view, (b) Top (angled) view.

3. RESULT AND DISCUSSION

Figure 5(a) shows a typical *I*-*V* curve for a green-emitting hybrid LED. The turn-on voltage is around 2.5 V, which is close to the bandgap energy observed in the PL spectrum (Fig. 2). The on-series resistance (R_s) is calculated via a linear

fit to the equation [19] $IdV/dI=R_sI+kT/e$ for $V \gg kT/e$ and determined to be 4.75 MΩ. This relatively high value is most likely due to (1) high contact resistance because the metal contacts to the *p*-GaN were not annealed and (2) the closeness (~70 nm) of the *p*-contact to GaN/AlN interface (Fig. 4(a)), which could lead to interface effects such as a two dimensional electron gas or elevated dislocation densities corrupting the Ohmic nature of the contact. R_s could be lowered through the use of a lower *p*-GaN etch depth to increase the separation between the contact and the GaN/AlN interface. The Ni/Au was not annealed to make a better Ohmic contact with the *p*-GaN because the ZnO surface morphology was observed to be modified by annealing at 500 °C.[18] Decreasing the *p*-GaN etch depth and annealing the *p*-contact could improve the forward-bias (FB) *I-V* characteristics. Under FB, green light was easily observed with the naked eye at RT under continuous-wave operation.

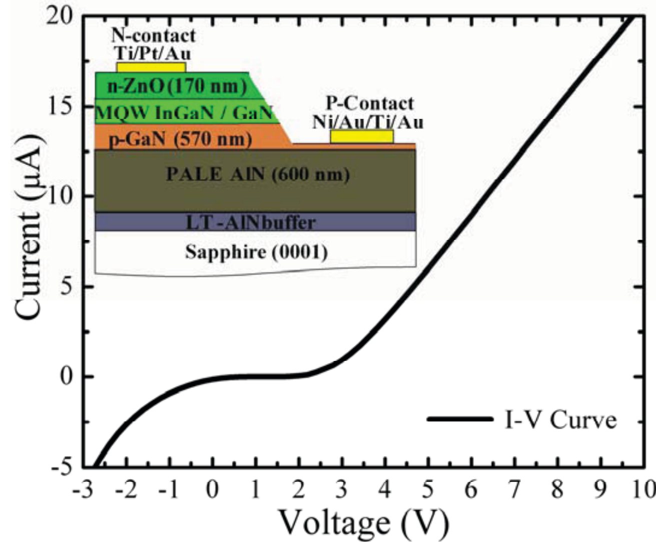

Fig. 5. *I-V* curve of the fabricated LED. The device structure is illustrated in the inset.

Reverse-bias characteristics are studied in ref [8]. As the *p*-GaN contact is close to the GaN/AlN interface, where there are many dislocations, a highly nonlinear increase in leakage current with respect to reverse-bias voltage was observed. The leakage current is known to be proportional to the square of the density of dislocations. [20] At high reverse bias, there is field-assisted thermal ionization of carriers from the defect-associated traps, which is known as Poole–Frenkel effect. Thus, the leakage current is expected to obey [21, 22]

$$I = I_0 \exp\left(\frac{\beta_{BF} E^{1/2}}{kT}\right). \quad (1)$$

The average electric field (E) dependence on the reverse bias (V) was found from $E=(V+V_i)/w$, where V_i is the built-in junction voltage and w is the depletion width.[21, 23] Figure 3(b) in ref [8] plots the best fit of Eq. (1) to our experimental data. From this fit, we obtain $\beta_{BF}=7.6\times10^{-4}$ eV $V^{1/2}$ $cm^{1/2}$. This value is slightly higher than for GaN(4.5×10^{-4} eV $V^{1/2}$ $cm^{1/2}$).[22] For higher density of dislocations, β_{BF} tends to be bigger.[20,21,22] Since leakage current scales with the square of the density of dislocations,[20] the effective density of dislocations was calculated to be 8.2×10^{-8} cm^{-2}. This theoretical fit shows that under reverse bias, hopping conduction is dominant in these hybrid LEDs similar to conventional *p-n* (In)GaN diodes.[21,22] Further optimization of the hybrid LED design and fabrication process are in progress.

Electroluminescence (EL) spectra were acquired for the LEDs under pulsed operation (duty cycle of 10% and frequency of 5 kHz) in order to reduce heating effects under high current injection (Fig. 6). The peak intensity was observed to depend linearly on the current density [Fig. 6(b)]. A blueshift from 510 to 504 nm was observed as the current increased from 400 to 1000 μA. The FWHM decreased simultaneously from 194 to 179 meV. These effects have been attributed to free-carrier screening of the piezoelectric field, which leads to bandgap renormalization. [24] The spectral narrowing for the device demonstrates no band-filling effects even for higher current injections and thus indicates superior quality

of the active layer. [25] This is consistent with the high compositional and structural integrities of the MQWs inferred from the XRD studies and can be attributed to the lower T_s employed for PLD of the ZnO top *n*-layer.

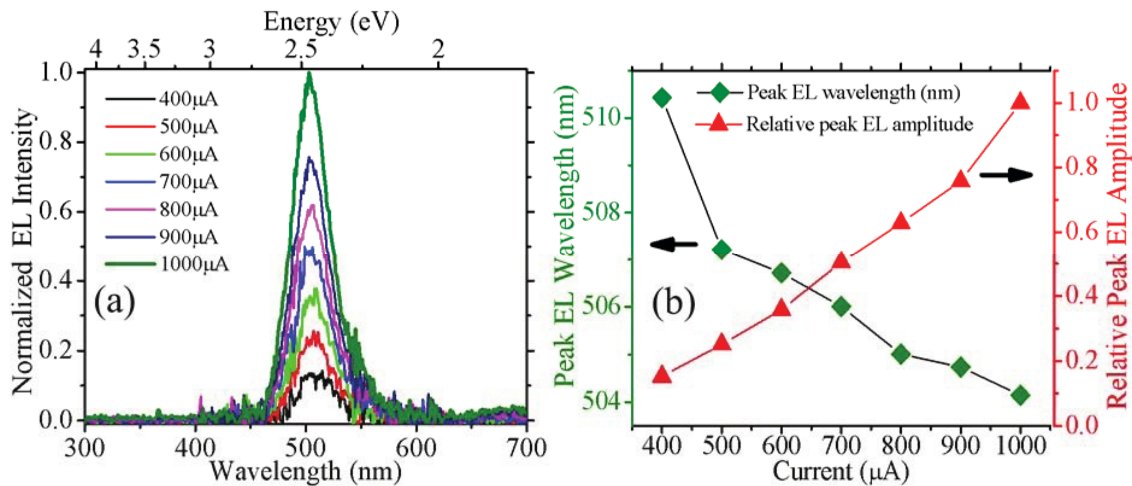

Fig. 6. (a) Normalized EL intensity of the hybrid green LED at RT. (b) Peak EL wavelength and amplitude with respect to injection current.

4. CONCLUSION

Novel hybrid green LEDs were developed. These devices employed an inverted *p*-*n* structure and the substitution of *n*-ZnO for the *n*-GaN layer. Conventional MOCVD growth was used for the *p*-GaN and MQWs. Lower temperature PLD was adopted for the ZnO growth in order to combat thermal degradation of the InGaN layers. High structural and optical quality of the ZnO, GaN and (In)GaN layers were confirmed using XRD and PL analyses, which suggested that the integrity of the MQW was maintained.

Under these processing conditions, a hybrid LED giving green EL between 510 and 504 nm, with a CW output on the order of μW, at RT was realized. Thermally induced degradation of the InGaN active layers was combated through the adoption of PLD for the ultimate (*n*-ZnO) growth step since significantly lower T_s was required than for the conventional MOCVD growth of GaN. Such an inverted hybrid structure approach could hold the prospect for the development of future green LEDs with superior performance. In addition, the inversion of the *p*-*n* junction such that the *n*-ZnO becomes the top layer, preserves the MQW and reduces the total internal reflection (which can improve light extraction).

5. FUTURE WORK

Hybrid LED output power is being enhanced via the device fabrication optimization. Particularly, *p*-GaN etch-depth is under investigation to inject holes more uniformly. Thicker green active layers are also being developed. As ZnO re-growth temperature (unlike GaN) is lower than that of MQW, thicker InGaN layers will be more stable in these hybrid LEDs and should lead to higher LED output power with better green spectrum quality.

REFERENCES

[1] Humphreys, C.J. , "Solid-State Lighting," MRS Bulletin 33, 459-470 (2008).

[2] Gardner, N.F., Muller, G.O., Shen, Y.C., Chen G., Watanabe S., Gotz W., and Krames, M.R., "Blue-emitting InGaN-GaN double-heterostructure light-emitting diode reaching maximum quantum efficiency above 200 A/cm^2," Appl. Phys. Lett. 91, 243506 (2007).

[3] Cho, Y.H., Lee S.K., Kwack H.S., Kim J.Y., Lim K.S., Kim H.M., Kang T.W., Lee S.N., Seon M.S. Nam O.H., and Park Y.J.," Carrier loss and luminescence degradation in green-light-emitting InGaN quantum wells with micron-scale indium clusters," Appl. Phys. Lett. 83, 2578 – 2580 (2003).
[4] Park I.K., Kwon M.K., Kim J.O, Seo S.B., Kim J.Y., Lim J.H., Park S.J., and Kim Y.S., "Green light-emitting diodes with self-assembled In-rich InGaN quantum dots," Appl. Phys. Lett. 91, 133105 (2007).
[5] Bayram C., Pau J.L., McClintock R., and Razeghi M., "Comprehensive study of blue and green multi-quantum-well light emitting diodes grown on conventional and lateral epitaxial overgrowth GaN" Applied Physics B, DOI: 10.1007/s00340-008-3321-y (2008).
[6] Ho I., and Stringfellow G.B., "Solid phase immiscibility in GaInN," Appl. Phys. Lett. 69, 2701-2703 (1996).
[7] Daele B., Van Tendeloo G., Jacobs K., Moerman I., and Leys M.R. , "Formation of metallic In in InGaN/GaN multiquantum wells," Appl. Phys. Lett. 85, 4379-4381 (2004).
[8] Bayram C., Teherani F.H., Rogers D., and Razeghi M., "A hybrid green light-emitting diode comprised of n-ZnO/(InGaN/GaN) multi-quantum wells/p-GaN," Appl. Phys. Lett. 93, 081111 (2008).
[9] Rogers D. J., Teherani F.H., Yasan A., McClintock R., Mayes K., Darvish S.R., Kung P., Razeghi M., and Garry G., "ZnO Thin Film Templates for GaN-based Devices," Proc. SPIE 5732, 412-416 (2005).
[10] An S.J., Chae J.H., Yi G.C., and Park G.H., "Enhanced light output of GaN-based light-emitting diodes with ZnO nanorod arrays," Appl. Phys. Lett. 92, 121108 (2008).
[11] Alivov Ya. I., Van Nostrand J.E., and Look D.C., "Observation of 430 nm electroluminescence from ZnO/GaN heterojunction light-emitting diodes," Appl. Phys. Lett. 83, 2943-2945 (2003).
[12] Rogers D.J., Teherani F.H., Yasan A., Minder K., Kung P., and Razeghi M.," Electroluminescence at 375 nm from a ZnO/GaN:Mg/c-Al_2O_3 heterojunction light emitting diode," Appl. Phys. Lett. 88, 141918 (2006).
[13] Rogers D. J., Teherani F. H., Kung P., Minder K., and Razeghi M., "Materials characterization of n-ZnO/p-GaN:Mg/c-Al2O3 UV LEDs grown by pulsed laser deposition and metal–organic chemical vapor deposition," Superlattices and Microstruct. 42, 322-326 (2007).
[14] Bayram C., Pau J.L., McClintock R., and Razeghi M., "Delta-doping optimization for high quality p-type GaN," Journal of Applied Physics 104, 083512 (2008).
[15] www.nanovation.com
[16] Bayram C., Pau J.L., McClintock R., and Razeghi M., "Performance enhancement of GaN ultraviolet avalanche photodiodes with p-type delta-doping," Appl. Phys. Lett. 92, 241103 (2008).
[17] Smith M., Chen G.D., Lin J.Y., Jiang H.X. Salvador A., Sverdlov B.N., Botchkarev A., Morkoc H., Goldenberg B., "Mechanisms of band-edge emission in Mg-doped p-type GaN," Appl. Phys. Lett. 68, 1883- 1885(1996).
[18] Bayram C., Teherani F.H., Rogers D., and Razeghi M., "Fabrication and Characterization of Novel Hybrid Green LEDs Based on Substituting n-type ZnO for n-type GaN in an Inverted p-n Junction," submitted (2009).
[19] Schubert E.F., [Light Emitting Diodes], Cambridge University Press, Cambridge, England, (2003).
[20] Li D.S., Chen H., Yu H.B., Jia H.Q., Huang Q., and Zhou J.M., "Dependence of leakage current on dislocations in GaN-based light-emitting diodes," J. Appl. Phys. 96, 1111-1114 (2004).
[21] Kuksenkov D.V., Temkin H., Osinsky A., Gaska R., and Khan M.A., "Origin of conductivity and low-frequency noise in reverse-biased GaN p-n junction," Appl. Phys Lett 72, 1365 – 1367 (1998).
[22] Ferdous M.S., Wang X., Fairchild M.N., and Hersee S.D. "Effect of threading defects on InGaN/GaN multiple quantum well light emitting diodes," Appl. Phys. Lett. 91, 231107 (2007).
[23] Sze S.M., [Physics of Semiconductor Devices, 2nd ed.],Wiley, New York, (1981).
[24] Takeuchi T., Wetzel C., Yamaguchi S., Sakai H., Amano H., and Akasaki I., "Determination of piezoelectric fields in strained GaInN quantum wells using the quantum-confined Stark effect," Appl. Phys. Lett. 73, 1691-1693 (1998).
[25] Qi Y.D., Liang H., Wang D., Lu Z.D., Tang W., and Lau K.M., "Comparison of blue and green InGaN/GaN multiple-quantum-well light-emitting diodes grown by metalorganic vapor phase epitaxy," Appl. Phys. Lett. 101903 (2005).